NEW CONSTRAINTS ON LUNAR HEAT FLOW RATES FROM LRO DIVINER LUNAR RADIOMETER EXPERIMENT POLAR OBSERVATIONS David A. Paige[1] dap@moon.ucla.edu, Matthew A. Siegler[2], [1]Department of Earth, Planetary and Space Sciences, UCLA, Los Angeles, CA 90095; [2]Planetary Science Institute, Tucson AZ 85619.

Introduction: The heat flow rate from the lunar interior is a fundamental property of the moon that is related to its composition, interior structure and history. Lunar heat flow rates have been measured at the Apollo 15 and 17 landing sites [1], but it is likely that the measured values of 21 mWm^{-2} and 14 mWm^{-2} respectively may not be representative of the moon as a whole due to the presence of enhanced radiogenic elements at these landing sites [2,3]. The Diviner Lunar Radiometer Experiment on the Lunar Reconnaissance Orbiter [4] has acquired an extensive set of thermal emission from the lunar surface at infrared wavelengths, including the first radiometric measurements of surface temperatures at the lunar poles [5]. Due to its low obliquity and rough topography, the moon has permanently shadowed cryogenic regions at high latitudes that never receive direct sunlight. The temperatures of the coldest of these regions can be used to place upper limits on the heat flow rate from the lunar interior because if other heat sources are neglected, then surface thermal emission is balanced by heat flow from warmer lunar interior [6].

Theory: The instantaneous heat balance of the surface can be represented as:

$$H_{solar} + H_{ir} + k\frac{dT}{dz} + F_{horiz} + F_{\uparrow} = F_{ir} = \varepsilon\sigma T^4$$

where H_{solar} is the surface heating rate due to the absorption of direct and scattered solar radiation, H_{ir} is the surface heating rate due to scattered infrared radiation, k is the thermal conductivity and dT/dz is the surface thermal gradient, F_{horiz} is the lateral conducted heat flux from warmer surrounding regions, $F_{\uparrow}$ is the heat flow rate from the interior, F_{ir} is the bolometric thermal emission from the surface, ε is the bolometric surface emissivity, σ is the Stefan-Boltzmann constant and T is the surface temperature. For the trivial case where H_{solar}, H_{ir} and F_{horiz} are zero, then the surface temperature will remain at a constant value and $F_{\uparrow}$ will equal F_{ir}. When surface temperatures are at an annual minima, all the terms in the equation will be positive, and therefore a measurement of F_{ir} can provide a useful upper limit for $F_{\uparrow}$ as long as H_{solar}, H_{ir}, $k\frac{dT}{dz}$ and F_{horiz} are small.

Observations. During the past 6 years, Diviner has acquired an unprecedented set of multispectral thermal emission measurements of the moon from low polar orbit. These measurements provide detailed characterizations of lunar polar temperatures and their diurnal and seasonal variability. We have examined the Diviner data at both poles to locate the coldest well-resolved region. We have identified an extremely cold region within an unnamed 3 km diameter impact crater (tentatively named "Region 5") located to the east of Haworth Crater centered at 87.0°S, 15.3°E (See Fig. 1,2).

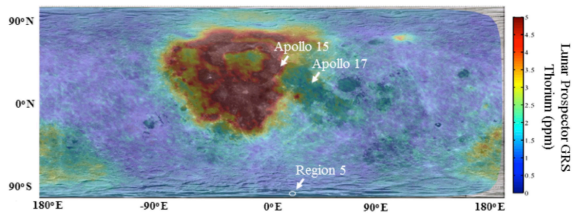

Fig. 1. Global lunar thorium abundance from Lunar Prospector data [7]. Heat flow measurements in Region 5 are not affected by the crustal enrichment in radiogenic elements associated with the PKT.

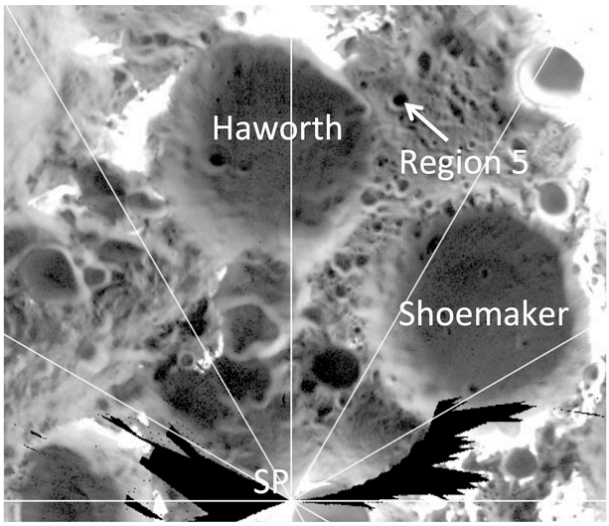

Fig. 2. Diviner multi-year Channel 8 brightness temperature map of the south polar region at midnight local time, showing the location of Region 5, an extremely cold unnamed crater that we use to constrain the lunar heat flow rate.

We collected all the Diviner Chanel 9 calibrated radiances for a circular area of radius 1.25 km centered on this crater and produced a time history of the radiance-weighted average brightness temperatures, T_9 (See Fig. 3). Diviner's Channel 9 covers a wavelength region from 100μm to beyond 400μm, and encom-

passes more than 80% of the bolometric thermal emission from a 20K blackbody. Since $F_{ir} \cong \sigma (T_9)^4$, the Diviner Channel 9 brightness temperature measurements map directly to F_{ir}, independent of the surface infrared emissivity. Each data point in Fig. 3 represents a unique LRO near-periapsis flyover of the region, providing Diviner with an IFOV of roughly 100m by 200m. Each data point represents the radiometric average of ~360 individual Diviner measurements, which boosts signal-to-noise by a factor of ~19 to yield a brightness temperature uncertainty of less than ±0.5K at 20K. Only passes with more than 200 IFOV's were considered valid. As shown in Fig. 3, the measured temperatures show a dominantly seasonal variation with an amplitude of ~25K, with annual minimum temperatures of ~18K. The lowest valid average temperatures were observed during the first winter were ~17.5K.

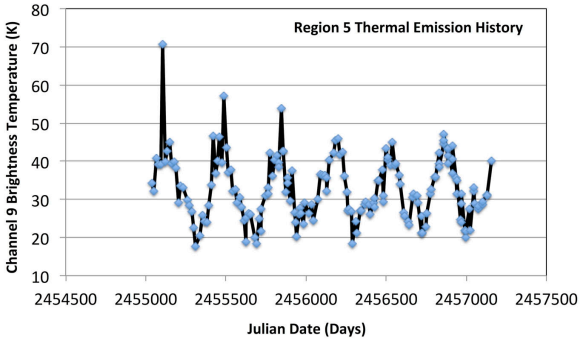

Fig. 3: Diviner measurements of Region 5 thermal history covering six years starting in July, 2009 and ending in December, 2015.

Analysis. We have used ray-tracing thermal model calculations [5] using a LOLA polar topographic grid with 120m spatial resolution to validate the temperature history trends shown in Fig. 3. The sharp summertime temperature peaks observed with decreasing amplitudes the first three years are due to the scattered radiation from adjacent directly illuminated areas. The warm spikes disappeared during subsequent years due to the 18.6-year precession of the lunar orbital plane. Given that the observed temperatures are not observed to "bottom out" at specific value, it appears that H_{solar}, H_{ir} and $k\frac{dT}{dz}$ never reached zero for this region, even at its coldest. However, if we assume that they are all zero, we can estimate an upper limit for the heat flow rate of $F_{\uparrow}$<6 mWm^{-2}. This limit is not directly affected assumptions regarding the infrared emissivity of the surface or the profile of thermal conductivity – both of which may differ significantly from those at warmer, lower latitudes.

Discussion. Fig. 4 shows the Diviner heat flow results for Region 5 compared with the two data points from Apollo. Diviner's significantly lower values measured near the south pole are consistent with the global distribution of the radiogenic element Thorium as measured by Lunar Prospector [7] (See Fig. 1). Based on GRAIL data, the lunar south polar region borders a region of low crustal thickness associated with the SPA basin [8]. Heat flow measurements in this area may therefore be more indicative of the abundance of radiogenic elements in the lunar mantle than in other areas of the moon [9]. The 6 mWm^{-2} value is near the lower limit of PKT region mantle heat flux estimated by [10] assuming 4.7× 10^{-9} Wm^{-3}, mantle heat production (as in [3]). As the crust in the polar regions is not likely to be fully devoid of radiogenic materials, this implies the PKT estimate of mantle heat production is higher than the global average. Assuming a feldspathic composition, the roughly 40km crust below Region 5 will itself supply ~3mWm^{-2}, resulting in a remaining mantle radiogenic heat production of 2.5 × 10^{-9} Wm^{-3} (equivalent to ~3.8ppb U), similar to the highly depleted mantle values estimated by [1]. This in turn would imply the remaining ~2× 10^{-9} Wm^{-3} of heat in the PKT region mantle [10] is not a result of radiogenic production, but rather due to a hypothesized warm mantle upwelling in this region [3,11].

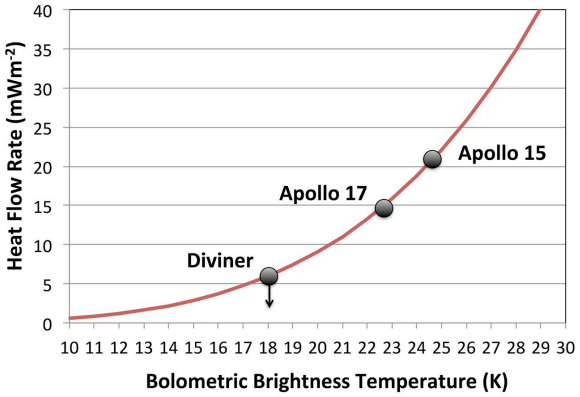

Fig. 4: Measured lunar heat flow rates and corresponding bolometric brightness temperatures.

References: [1] Langseth, M. G. et al, Proc. Lunar Sci. Conf, 7th, 3143-3171, 1976. [2] Warren, P. H. and K. K. L. Rasmussen, JGR 92, 3453-3465, 1987. [3] Wieczorek, M. A. and R. J. Phillips, JGR 105, 20,417-20,430, 2000. [4] Paige, D. A. et al, Space Sci. Rev, 150:125-160, 2010. [5] Paige, D. A. et al., Science, 330 479-482 2010. [6] Watson, K. JGR 72, 3301-3302, 1967. [7] Lawrence, D. J. et al., Science 281, 1484-1489, 1998. [8] Wieczorek, M. A. et al. Science 339, 671-675, 2012. [9] Kiefer, W. S. Planet. Space Sci. 60, 155-165, 2012. [10] Siegler and Smrekar, JGR 119, 2014. [11] Laneuville, M. JGR 118, 1435–1452, 2013.